Hindawi
Mathematical Problems in Engineering
Volume 2017, Article ID 9485127, 15 pages
https://doi.org/10.1155/2017/9485127

Research Article

A Multiobjective Robust Scheduling Optimization Mode for Multienergy Hybrid System Integrated by Wind Power, Solar Photovoltaic Power, and Pumped Storage Power

Lihui Zhang, He Xin, Jing Wu, Liwei Ju, and Zhongfu Tan

North China Electric Power University, Beijing 102206, China

Correspondence should be addressed to Liwei Ju; 183758841@qq.com

Received 28 February 2017; Revised 11 May 2017; Accepted 3 July 2017; Published 16 August 2017

Academic Editor: Huanqing Wang

Wind power plant (WPP), photovoltaic generators (PV), cell-gas turbine (CGT), and pumped storage power station (PHSP) are integrated into multienergy hybrid system (MEHS). Firstly, this paper presents MEHS structure and constructs a scheduling model with the objective functions of maximum economic benefit and minimum power output fluctuation. Secondly, in order to relieve the uncertainty influence of WPP and PV on system, robust stochastic theory is introduced to describe uncertainty and propose a multiobjective stochastic scheduling optimization mode by transforming constraint conditions with uncertain variables. Finally, a 9.6 MW WPP, a 6.5 MW PV, three CGT units, and an upper reservoir with 10 MW·h equivalent capacity are chosen as simulation system. The results show MEHS system can achieve the best operation result by using the multienergy hybrid generation characteristic. PHSP could shave peak and fill valley of load curve by optimizing pumping storage and inflowing generating behaviors based on the load supply and demand status and the available power of WPP and PV. Robust coefficients can relieve the uncertainty of WPP and PV and provide flexible scheduling decision tools for decision-makers with different risk attitudes by setting different robust coefficients, which could maximize economic benefits and minimize operation risks at the same time.

1. Introduction

WPP and PV are incapable of being accurately forecasted, stochastic, and unstable, making wind power and photovoltaic power not being used effectively and power output fluctuations. Abandoning wind and photovoltaic power phenomenon is getting more serious, which results in a waste of wind and light power and a great economic loss of enterprises. The hydropower reserves and installed capacity of China rank first in the world. Hydropower stations have the advantages of flexible starting and stopping, high speed of loading up and down, and low operation and maintenance costs [1] and can adapt to the rapid change of the grid load. Pumped storage power station is the most mature economic power to sharp peak and fill valley. The hybrid generation system is composed of wind, photovoltaic, and pumped storage power. This system can smooth the output of wind power and photovoltaic power and reduce the benefit losses brought by the intermittent and stochastic of wind power and photovoltaic power, so that the grid accommodation capacity for wind and PV power can be improved [2]. Researches on how to coschedule WPP, PV, and PHSP can effectively solve the power supply contradiction in intermittent energy operating and narrow down problems like difficulties in grid connection, power limitation, and market accommodation capacity [3] and finally have great economics and sustainable developing significance in reducing the electric power system uncertainty risk and improving economic benefits.

Current researches on power system scheduling optimization method considering WPP and PV grid connection mainly focus on the stochastic scheduling model construct. Literature [4] introduced a new general equation for power system economic scheduling model, considering conventional thermal units, wind turbine generators, and changing characteristics of wind speed and power demand. The influence the dynamic cost coefficients have on system

operation costs has been analyzed in a simple testing system. Literature [5] established a stochastic optimization model for wind and thermal power economic scheduling based on the analysis of wind power stochastic output and calculated the possible extra costs in stabilizing power system caused by unstable wind power. Literature [6] considered power supplying reliability of the wind-photovocait grid-connecting generation system and aimed at realizing system minimum power consumption. Then, a wind-photovocait capacity combination to minimize system cost was proposed. The proposed models and methods study wind and PV connected to the grid and choose thermal power scheduling to stabilize wind power output. However, conventional thermal power units have high cost and limitations in peak regulation. Lower costs and ideal stabilizing effect are hard to achieve by CGT, WPP, and PV hybrid operation only.

Due to the rapid starting up and flexibility advantages of PHSP, many countries have studied the joint operation scheme and calculation and analysis model of uncertain renewable energy resources and pumped storage power stations with the regulation ability [7]. Literature [8] introduced the fact that PHSP is now seen as the most effective energy storage technology to improve the penetration ability of renewable energy and presented the operation mode of WPP-PHSP hybrid system to improve the wind power penetration ability. Literature [9] analyzed optimal scheduling WPP and PHSP cooperation and uncoordinated operation in energy and ancillary services market. New methods to model, simulate, and evaluate WPP and PHSP units were raised to increase system profits and VaR (value at risk). By optimizing WPP and PHSP utilization level, maximizing WPP and PHSP generation in simulation is taken as objective function in literature [10], so that the WPP reliability assessment methods are optimized as well. Literature [11] used WPP and PHSP cooperation to relieve the wind generation fluctuation influence to grids and proposed a reliability assessment method of Wind-Hydro integrated power system. Literature [12] developed a quantitative assessment model considering valley electric price, Wind-Hydro integrated power system, and energy conversion efficiency. In addition, the paper studied the influence the pumped storage power station has on wind power valley filling and peak-shaving in Wind-Hydro integrated power system. In order to lower the unbalanced costs of electricity market predicting wind power generation errors, literature [13] proposed WPP-PHSP integrated operation plan aiming at minimizing costs. The operation plan was modeling and quantifying wind power prediction uncertainty and optimized wind power utilization and pumped storage power. In literature [14], pumped storage system was used in photovoltaic technology. Based on system reliability and economic standards, literature [15] discussed the PV-Hydro cooperation system model and designed a reliability evaluation model. The research shows cooperation system improves the reliability of PV grid-connecting and, to a great extent, can improve the utilization rate of photovoltaic system, reducing abandoned electricity phenomenon. Literature [16] proposed a WPP-PV-Hydro hybrid generation system including wind power, PV, and hydro generation subsystems. Based on establishing the hybrid generation system, the paper analyzed three different operation plans.

Based on the above analysis, scholars at home and foreign countries have already carried out deep researches on the optimization scheduling of WPP, PV, and PHSP. Some literatures have already discussed the complementary effect of different clean energy, especially, WPP, PV, and PHSP. However, there are still some insufficient problems: firstly, the existing researches have not considered the optimization scheduling problems for decision-maker with different risk attitude. Since the uncertainty of WPP and PV will have great influence on system safe operation, which may bring great risk, therefore, the optimal scheme will change for decision-maker with different risk attitude; correspondingly, the output of WPP, PV, and PHSP will also change. Secondly, other literatures only study the optimization of the multienergy hybrid system (MEHS) under the maximum economic benefit without considering the risk cost. Under the premise of maximizing the consortium interests, it is important to consider the peaking effect and rotation reserve role of the pumped storage power station and how to coordinate with the gas turbine unit to enhance system stability and efficiency. Finally, little literatures are related to the researches on the optimization scheduling of MHES integrated by WPP, PV, PHSP, and cell-gas turbine (CGT). Reserve service is necessary for system safe operation since the output of WPP and PV is uncertainty. The peaking effect and rotation reserve role of PHSP should be considered and how to coordinate with the gas turbine unit to enhance system stability and efficiency should also be negligence. Therefore, the paper introduces the robust stochastic optimization theory [17] to handle the constraint conditions with stochastic variables by introducing robust coefficients, which could provide a flexible risk control tool for decision-maker with different risk attitudes. WPP, PV, CGT, and PHSP are integrated into MEHS with two optimization objective functions, namely, the maximum economic benefits and the minimum output fluctuation. The optimization effect of CGT on system stability and efficiency is also considered. PHSP is used as the energy storage equipment for reducing the uncertainty impact and improving the utilization efficiency of renewable energy. All above analysis motivates us to put forward a risk aversion model for MEHS system scheduling. The main contributions of this work are summarized as follows:

(i) The basic structure of multienergy complementary system and power output model are established. In order to achieve the maximum system economic efficiency and the minimum the fluctuation and consider the limitations of system operation, the multienergy complementary scheduling optimization model is presented. The model provides basic foundation for analysis the optimization function of pumped storage power plant and robust stochastic optimization theory.

(ii) The uncertainty description method for WPP and PV are proposed based on the Rayleigh distribution and the Beta distribution function. A stochastic optimization model for MEHS scheduling is designed based

on the robust stochastic theory with two objective functions of the maximum economic benefits and the minimum system output fluctuation. The robust coefficient is introduced to transform the constraint conditions with uncertain variables and reflect the risk attitude of decision-maker.

(iii) The simulation system consisted of 9.6 MW WPP, 6.5 MW PV, three CGT units, and an upper reservoir with equivalent capacity of 10 MW·h which is used to analyze the proposed model. According to the fluctuation of system economic benefits and unit output scheme under different robust coefficients, the optimal weight coefficient of objective function is determined. The effectiveness analysis of the robust stochastic optimization theory, the operational benefit analysis, and the sensitivity analysis of the pumped storage power station are carried out.

The remainder of this paper is organized as follows: Section 2 proposes basic results of the hybrid energy system and power output power model including WPP, PV, and PHSP. In Section 3, a scheduling optimization model for multienergy hybrid system is constructed with the objective functions of the maximum system economic operation and the minimum output fluctuations with constraint conditions of supply and demand balance, unit power generation, pumped storage power station operation, and system spins reserve. In Section 4, robust stochastic theory is introduced to construct scheduling model for MEHS system by handling with the constraint conditions with stochastic variables. The operation benefit analysis and sensitivity analysis for PHSP are set up to demonstrate the validity of the proposed model in Section 5. Section 6 highlights the main conclusions of this study.

2. Multienergy Complementary System Output Model

2.1. Multienergy Complementary System Structure. In this paper, wind power plant (WPP), photovoltaic generator (PV), cell-gas turbine (CGT), and pumped storage power station (PHSP) are integrated into a multienergy complementary system. Figure 1 shows system structure. In the multienergy complementary system, WPP and PV are mainly used to meet the load demand. When power generation of WPP and PV is more than system load demand, under the premise of satisfying system safe operation, surplus electricity is used for PHSP to pump water up to the upper reservoir. When the available power of WPP and PV is less than system load demand, PHSP will be scheduled to meet load demand. At the same time, in order to strengthen system safety and reliability and ensure system load to be guaranteed in poor water period, poor wind period, and low solar radiation period, CGT units can provide system reserve capacity in WPP and PV fluctuation time. In addition, CGT units can generate power to meet the load demand when the WPP, PV, and PS units cannot meet load demand [18]. The multienergy complementary operation integrated by WPP, PV, PHSP, and CGT units can both ensure the safe and reliable system operation and guarantee system load balance at the same time.

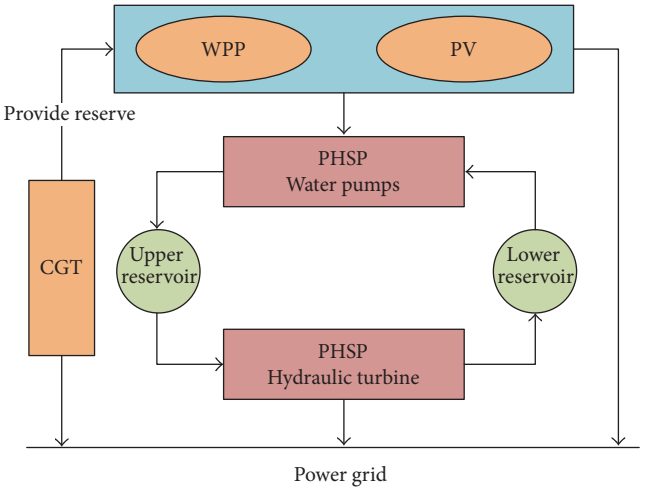

Figure 1: Multienergy complementary system structure.

2.2. Power Supply Output Power Model. In the proposed multienergy hybrid system, power supplies mainly include WPP, PV, PHSP, and CGT units. This chapter introduces the power output models of wind power, photovoltaic, and pumped storage power station.

2.2.1. Wind Power Output Power Model. For wind power plants, power output depends mainly on natural wind speed. Due to the stochastic characteristic of natural wind, power output is random. Some probability distributions, that is, the exponential distribution and the Gaussian distribution, are usually employed to model the stochastic disturbances. Literature [19] comparatively analyzed and evaluated the application of the Weibull distribution, Rayleigh distribution, Gamma distribution, and Lognormal distribution, which showed Rayleigh distribution could be better for simulating the distribution of wind speed. Therefore, Rayleigh distribution function is used to describe wind speed distribution, as

$$f(v) = \frac{\varphi}{\vartheta}\left(\frac{v}{\vartheta}\right)^{\varphi-1} e^{-(v/\vartheta)^{\varphi}}, \tag{1}$$

wherein v is real-time wind speed. φ, ϑ are shape parameter and scale parameter. Equation (1) is used to obtain the expectation and variance of wind speed distribution. Real-time output power of wind power plant can be calculated as

$$g^{*}_{W,t} = \begin{cases} 0, & 0 \le v_t < v_{\text{in}},\ v_t > v_{\text{out}}, \\ \dfrac{v_t - v_{\text{in}}}{v_{\text{rated}} - v_{\text{in}}} g_R, & v_{\text{in}} \le v_t \le v_{\text{rated}}, \\ g_R, & v_{\text{rated}} \le v_t \le v_{\text{out}}, \end{cases} \tag{2}$$

$$0 \le g_{W,t} \le g^{*}_{W,t},$$

wherein v_t is the real-time wind speed of WPP at time t; v_{in}, v_{rated}, and v_{out} are, respectively, the cut-in wind speed, rated wind speed, and cut-out wind speed.

2.2.2. PV Output Power Model. For photovoltaic generation units, output power is determined by solar radiation intensity. As literature [20] proved, Beta distribution function is used to describe solar radiation intensity as

$$f(\theta) = \begin{cases} \dfrac{\Gamma(\alpha)\Gamma(\beta)}{\Gamma(\alpha)+\Gamma(\beta)}\theta^{\alpha-1}(1-\theta)^{\beta-1}, & 0 \le \theta \le 1,\ \alpha \ge 0,\ \beta \ge 0, \\ 0, & \text{otherwise}, \end{cases} \tag{3}$$

wherein θ is solar radiation; α and β are the shape parameters of Beta distribution. After obtaining the expectation and variance of solar radiation intensity, α and β can be calculated as

$$\begin{aligned} \beta &= (1-\mu) \times \left(\frac{u \times (1+\mu)}{\sigma^2} - 1 \right), \\ \alpha &= \frac{\mu \times \beta}{1-u}, \end{aligned} \tag{4}$$

wherein u and σ are, respectively, the expectation and standard deviation of solar radiation intensity. After plugging (4) into (3), the solar radiation intensity distribution function can be obtained. Then, PV output power at time t can be calculated by photoelectric conversion function:

$$g^*_{\text{PV},t} = \eta_{\text{PV}} \times S_{\text{PV}} \times \theta_t, \quad 0 \le g_{\text{PV},t} \le g^*_{\text{PV},t}, \tag{5}$$

wherein η_{PV} and S_{PV} are solar radiation area and efficiency; θ_t is the solar radiation intensity at time t.

2.2.3. PHSP Output Power Model. Pumped storage power station includes two operating conditions, water storing and water inflowing to generate power. When electricity power is in short supply, usually peak time, electricity price is higher. At this time, pumped storage power station inflows to generate power to meet load demand and obtain profits. When electricity power is oversupply, usually valley time, electricity price is lower. Pumped storage power station stores water, and electricity costs are relatively lower at this time.

(1) Water Storage Operation Condition. The power of pumped storage power station is determined by pump installed capacity, pumping efficiency, and the reservoir storage capacity as

$$g_P^{\text{PS,min}} \le g_{P,t}^{\text{PS}} \le \left(g_P^{\text{PS,max}}, \frac{E^{\max} - E_t}{\eta_P \Delta t} \right), \tag{6}$$

wherein $g_{P,t}^{\text{PS}}$ is the power of pumped storage power station at time t; $g_P^{\text{PS,min}}$ and $g_P^{\text{PS,max}}$ are the lower and upper bound of pumping power; η_P is the pumping efficiency of pumped storage station; $E^{\max}$ is the maximum energy storage pumped storage power station; E_t is the energy storage at time t.

(2) Water Inflowing Operation Condition. The generation power of pumped storage power station is decided by installed capacity, generating efficiency, and reservoir energy storage size:

$$g_H^{\text{PS,min}} \le g_{H,t}^{\text{PS}} \le \min \left(g_H^{\text{PS,max}}, \frac{\left(E_t - E^{\min}\right)}{\Delta t} \eta_H \right), \tag{7}$$

wherein $g_{H,t}^{\text{PS}}$ is the inflowing generation power of pumped storage power station at time t; $g_H^{\text{PS,min}}$ and $g_H^{\text{PS,max}}$ are lower and upper bound of generating power; η_H is power generation efficiency of pumped storage power station; $E^{\min}$ is the minimum energy storage of pumped storage power station; E_t is the energy storage at time t.

3. Scheduling Operation Mode for Multienergy Complementary System

A multienergy complementary system integrated by clean energy generator units, gas generator units, and energy storage system is proposed in this paper. In model constructing, system security operating constraints and the overall system operating efficiency level should be considered. In the state of the optimal operation, maximizing system economic efficiency and environmental benefits should be achieved at the same time.

3.1. Objective Function. In the proposed multienergy complementary system component of WPP, PV, CGT, and PHSP, two optimization targets should be considered: maximizing system economic benefits and minimizing system output fluctuation. The former is set as the optimization target of multienergy complementary system; the latter objective function is set as the optimization target of the main grid.

(1) Maximizing System Economic Benefits. The economic benefit of the multienergy complementary system is mainly composed of four parts: wind power generation income, PV power generation profit, operating income of pumped storage power station, and gas turbine power generation. Specific objective function is as follows:

$$\max \quad R = \sum_{t=1}^{T} \left(R_{W,t} + R_{\text{PV},t} + R_{\text{CGT},t} + R_{\text{PS},t} \right), \tag{8}$$

wherein $R_{W,t}$, $R_{\text{PV},t}$, $R_{\text{CGT},t}$, and $R_{\text{PS},t}$ are, respectively, the generation profits of WPP, PV, CGT, and PS at time t, as (9)-(10):

$$R_{W,t} = \rho_{W,t} g_{W,t}, \tag{9}$$

$$R_{\text{PV},t} = \rho_{\text{PV},t} g_{\text{PV},t}, \tag{10}$$

$$R_{\text{PS},t} = \rho_{\text{PS},t}^{H} g_{\text{PS},t}^{H} - \rho_{\text{PS},t}^{P} g_{\text{PS},t}^{P}, \tag{11}$$

$$R_{\text{CGT},t} = \rho_{\text{CGT},t} g_{\text{CGT},t} - \pi_{\text{CGT},t}^{\text{pg}} - \pi_{\text{CGT},t}^{\text{ss}}. \tag{12}$$

In (12), $\pi^{pg}_{CGT,t}$ and $\pi^{ss}_{CGT,t}$ are, respectively, the generation cost and startup-shutdown cost of CGT at time t.

$$\begin{aligned}
\pi^{pg}_{CGT,t} &= a_{CGT} + b_{CGT} g_{CGT} + c_{CGT} \left(g_{CGT,t}\right)^2, \\
\pi^{ss}_{CGT,t} &= \left[u_{CGT,t}\left(1 - u_{CGT,t}\right)\right] D_{CGT,t}, \\
D_{CGT,t} &= \begin{cases} N^{hot}_{CGT}, & T^{min}_{CGT} < T^{off}_{CGT,t} \le T^{min}_{CGT} + T^{cold}_{CGT}, \\ N^{cold}_{CGT}, & T^{off}_{CGT,t} > T^{min}_{CGT} + T^{cold}_{CGT}, \end{cases}
\end{aligned} \tag{13}$$

wherein a_{CGT}, b_{CGT}, and c_{CGT} are, respectively, the generation cost coefficients of CGT unit and can be obtained by generation historical data regression. g_{CGT} is the generation power of CGT at time t. $u_{CGT,t}$ is the operation status of CGT at time t, a binary variable. $u_{CGT,t} = 1$ means CGT is in operation, whereas $u_{CGT,t} = 0$ means CGT is not in operation. $D_{CGT,t}$ is the startup/shutdown costs of CGT unit. N^{hot}_{CGT} and N^{cold}_{CGT} are, respectively, the hot start costs and cold start costs of CGT unit. T^{min}_{CPP} is the minimum allowable downtime of CGT. $T^{off}_{CGT,t}$ is the continuous downtime of CGT at time t. T^{cold}_{CPP} is cold startup time of CGT. $T^{off}_{CGT,t}$ is the downtime of CGT unit.

(2) Minimizing MEHS Output Fluctuation. As wind power and photovoltaic power generation have intermittent and fluctuating characteristics, the large-scale wind power and photovoltaic power generation connecting to the main grid will affect the power grid normal operation. Therefore, for main grid, minimizing system load fluctuation should be the operating optimization objectives. The specific objective function is as follows:

$$\begin{aligned}
\min \quad N &= \left\{ \sum_{t=1}^{T} \frac{\left[g_{W,t} + g_{PV,t} - \left(g^{P}_{PS,t} - g^{H}_{PS,t}\right) - g_{av}\right]^2}{T} \right\}^{1/2}, \qquad (14) \\
g_{av} &= \sum_{t=1}^{T} \frac{\left[g_{W,t} + g_{PV,t} - \left(g^{P}_{PS,t} - g^{H}_{PS,t}\right)\right]}{T}, \qquad (15)
\end{aligned}$$

wherein N is the standard deviation of WPP and PV generation output power fluctuation, also named as WPP and PV output fluctuation function; T is system scheduling cycle; g_{av} is the average system output power. The pumped storage power station mainly uses WPP and PV generation to pump water and store energy. Therefore, as N is smaller, indicating a smaller fluctuation in WPP and PV output power, it is more favorable to system operation safety.

3.2. Constraint Conditions. The multienergy complementary system is component of WPP, PV, CGT, and PHSP. Therefore, system supply and demand balance constraints, WPP, PV, and CGT generating power constraints, pumped storage power station operation constraints, and system rotation reserve constraints are considered.

(1) Supply and Demand Balance Constraint

$$\underbrace{g_{W,t}\left(1 - \varphi_W\right) + g_{PV,t}\left(1 - \varphi_{PV}\right) + \left(\rho^{H}_{PS,t} g^{H}_{PS,t} - \rho^{P}_{PS,t} g^{P}_{PS,t}\right) + g_{CGT,t}\left(1 - \varphi_{CGT}\right)}_{\text{MEHS output}} + g_{GC,t} = L_t, \tag{16}$$

wherein φ_W, φ_{PV}, and φ_{CGT} are power loss rate of WPP, PV, and CGT, respectively. $g_{GC,t}$ is power output of system purchasing from generation company.

(2) CGT Operation Constraints. CGT operation constraints mainly include power generation constraints, unit climbing constraints, and unit start-stop time constraints, as

$$u_{CGT,t} g^{min}_{CGT} \le g_{CGT,t} \le u_{CGT,t} g^{max}_{CGT}, \tag{17}$$

$$u_{CGT,t} \Delta g^{-}_{CGT} \le g_{CGT,t} - g_{CGT,t-1} \le u_{CGT,t} \Delta g^{+}_{CGT}, \tag{18}$$

$$\left(T^{on}_{CGT,t-1} - M^{on}_{CGT}\right)\left(u_{CGT,t-1} - u_{CGT,t}\right) \ge 0, \tag{19}$$

$$\left(T^{off}_{CGT,t-1} - M^{off}_{CGT}\right)\left(u_{CGT,t} - u_{CGT,t-1}\right) \ge 0, \tag{20}$$

wherein g^{max}_{CGT} and g^{min}_{CGT} are the upper and lower limitation of CGT, respectively. Δg^{+}_{CPP}, Δg^{-}_{CPP} are the upper and lower limitation of CGT, respectively. M^{on}_{CGT} and M^{off}_{CGT} are the minimum startup time and the minimum shutdown time of CGT, respectively. $T^{on}_{CGT,t-1}$ and $T^{off}_{CGT,t-1}$ are the continuous operation time and the continuous shutdown time of CGT at time $t - 1$, respectively. Equation (17) is generator power constraint; (18) is unit climbing constraint; (19) and (20) are system startup/shutdown time constraints.

(3) Pumped Storage Power Station Operation Constraints. Pumped storage power station constraints include the energy storage balance constraints, capacity constraints, pumping capacity constraints, and output power constraints, as

$$E_t = E_{t-1} + \eta_P g^{P}_{PS,t} \Delta t - \frac{g^{H}_{PS,t} \Delta t}{\eta_H}, \tag{21}$$

$$\begin{aligned}
\frac{E_0 - E^{max}}{\eta_P} &\le \frac{\sum_{t=1}^{T'} g^{H}_{PS,t} \eta_H}{\eta_P} - \sum_{t=1}^{T'} g^{P}_{PS,t} \\
&\le \frac{E_0 - E^{min}}{\eta_P},
\end{aligned} \tag{22}$$

$$\frac{\sum_{T' \in T} g^{H}_{PS,t} \eta_H}{\eta_P} = \sum_{T' \in T} g^{P}_{PS,t}, \tag{23}$$

$$K^{P}_{PS,t} g^{P,min}_{PS,t} \le g^{P}_{PS,t} \le K^{P}_{PS,t} g^{P,max}_{PS,t}, \tag{24}$$

$$K^{H}_{\mathrm{PS},t} g^{H,\min}_{\mathrm{PS},t} \le g^{H}_{\mathrm{PS},t} \le K^{H}_{\mathrm{PS},t} g^{H,\max}_{\mathrm{PS},t}, \tag{25}$$

$$K^{P}_{\mathrm{PS},t} + K^{H}_{\mathrm{PS},t} \le 1, \tag{26}$$

wherein E_0 is the initial water quantity in upper and lower reservoir of pumped storage power station, and $T' \in T$; $K^{P}_{\mathrm{PS},t}$ is the energy storage state variable and is 0-1 variable, 1 meaning the station is in energy storing, or the station is not. $K^{H}_{\mathrm{PS},t}$ is the generation state variable, 0-1 variable. 1 means that the power plant is in power generating state; otherwise the power plant is not. In order to ensure the pumped storage power station operating safely, the pumping water condition and inflowing condition are set not to operate at the same time as (26) shows. Equation (22) represents the energy storage balance constraints, and (23) is the pumped storage power generation constraint. Equations (24) and (25) are, respectively, the pumping power constraint and discharge power constraint.

(4) System Reserve Constraints

$$\begin{aligned}
&\left(g^{\max}_{\mathrm{CGT},t} - g_{\mathrm{CGT},t}\right) + \left(g^{H,R}_{\mathrm{PS}} - g^{H}_{\mathrm{PS},t}\right) + g_{W,t} + g_{\mathrm{PV},t} \\
&\quad \ge R_L L_t + R_{W,t} g_{W,t} + R_{\mathrm{PV},t} g_{\mathrm{PV},t}, \\
&\left(g_{\mathrm{CGT},t} - g^{\min}_{\mathrm{CGT},t}\right) + \left(g^{H}_{\mathrm{PS},t} - g^{H,\min}_{\mathrm{PS}}\right) \\
&\quad \le R_L L_t + R_W g^{*}_{W,t} + R_{\mathrm{PV},t} g^{*}_{\mathrm{PV},t},
\end{aligned} \tag{27}$$

wherein $g^{H,R}_{\mathrm{PS}}$ is rated power of pumped storage; R_L is the rotation reserve ratio, usually 5%; $R_{W,t}$ and $R_{\mathrm{PV},t}$ are, respectively, the increased rotation reserve ratio caused by the access of WPP and PV, and the values are equal to the relative error of WPP and PV generation forecast. (Due to the random fluctuation of WPP and PV generation and the low accuracy of forecasting, it is necessary to keep sufficient reserve to balance the deviation between the real generation and forecasting generation of WPP and PV). Considering the WPP and PV prior accessing policy, only take the amount of abandoned WPP and PV electricity as positive spares; that is, when power output is insufficient, the wind power will be reput without considering a negative spare.

4. A Robust Scheduling Optimization Mode for MEHS

4.1. Descriptions for WPP and PV Uncertainty. In the proposed MEHS, WPP and PV output power have intermittent and volatility characteristics. In reality, WPP and PV generation output power cannot be accurately simulated and predicted, but this problem can be overcome by predicting results, as (28).

$$\begin{aligned}
\widetilde{g}_{W,t} &= g_{W,t} + \eta_{W,t} e_{W,t} g_{W,t}, \quad \eta_{W,t} \in [-1, 1], \\
\widetilde{g}_{\mathrm{PV},t} &= g_{\mathrm{PV},t} + \eta_{\mathrm{PV},t} e_{\mathrm{PV},t} g_{\mathrm{PV},t}, \quad \eta_{\mathrm{PV},t} \in [-1, 1],
\end{aligned} \tag{28}$$

wherein $\widetilde{g}_{W,t}$ and $\widetilde{g}_{\mathrm{PV},t}$ are, respectively, the uncertainty forms of WPP and PV generation; $g_{W,t}$ and $g_{\mathrm{PV},t}$ are, respectively, the predictive value of WPP output power and the predictive value of PV output power; $\rho_{W,t}$ and $\rho_{\mathrm{PV},t}$ are, respectively, the estimation error coefficients of WPP and PV generating; $\eta_{W,t}$ and $\eta_{\mathrm{PV},t}$ are the error direction coefficients in WPP and PV generation prediction.

4.2. The Robust Scheduling Optimization Model. According to (28), WPP and PV generator output power, respectively, belong to $[(1 - e_{W,t}) \cdot g_{W,t}, (1 + e_{W,t}) \cdot g_{W,t}]$ and $[(1 - e_{\mathrm{PV},t}) \cdot g_{\mathrm{PV},t}, (1 + e_{\mathrm{PV},t}) \cdot g_{\mathrm{PV},t}]$. This interval effectively covers the WPP and PV generation fluctuating possibility. At the same time, in order to ensure the feasible solution existence, the load balance between supply and demand (see (16)) needs to be corrected:

$$\underbrace{g_{W,t}\left(1 - \varphi_W\right) + g_{\mathrm{PV},t}\left(1 - \varphi_{\mathrm{PV}}\right) + \left(\rho^{H}_{\mathrm{PS},t} g^{H}_{\mathrm{PS},t} - \rho^{P}_{\mathrm{PS},t} g^{P}_{\mathrm{PS},t}\right) + g_{\mathrm{CGT},t}\left(1 - \varphi_{\mathrm{CGT}}\right)}_{\text{MEHS output}} + g_{\mathrm{GC},t} \ge L_t. \tag{29}$$

Set N_t as system load demand, as

$$\begin{aligned}
N_t = &\left(\rho^{H}_{\mathrm{PS},t} g^{H}_{\mathrm{PS},t} - \rho^{P}_{\mathrm{PS},t} g^{P}_{\mathrm{PS},t}\right) + g_{\mathrm{CGT},t}\left(1 - \varphi_{\mathrm{CGT}}\right) \\
&+ g_{\mathrm{GC},t} - L_t.
\end{aligned} \tag{30}$$

Plug (30) into (29):

$$\begin{aligned}
&- \left[g_{W,t}\left(1 - \varphi_W\right) \pm e_{W,t} \cdot g_{W,t}\right] \\
&\quad - \left[g_{\mathrm{PV},t}\left(1 - \varphi_{\mathrm{PV}}\right) \pm e_{\mathrm{PV},t} \cdot g_{\mathrm{PV},t}\right] \le H_t.
\end{aligned} \tag{31}$$

Equation (31) shows there is a positive correlation between the strictness and the stochastic characteristic of the uncertainty constraints. To ensure that the constraints above are met when the actual output power of WPP and PV is close to the forecast boundary, auxiliary variables $\theta_{W,t}, \theta_{\mathrm{PV},t}$ ($\boldsymbol{\theta} \ge 0$) are introduced to strengthening (31):

$$\begin{aligned}
\theta_{W,t} &\ge \left|g_{W,t}\left(1 - \varphi_W\right) \pm e_{W,t} \cdot g_{W,t}\right|, \\
\theta_{\mathrm{PV},t} &\ge \left|g_{\mathrm{PV},t}\left(1 - \varphi_{\mathrm{PV}}\right) \pm e_{\mathrm{PV},t} \cdot g_{\mathrm{PV},t}\right|.
\end{aligned} \tag{32}$$

Then, (32) could be revised by considering (31) as follows:

$$\begin{aligned}
&- \left(g_{W,t} + e_{W,t} g_{W,t}\right) - \left(g_{\mathrm{PV},t} + e_{\mathrm{PV},t} g_{\mathrm{PV},t}\right) \\
&\quad \le -g_{W,t} + e_{W,t} g_{W,t} - g_{\mathrm{PV},t} + e_{\mathrm{PV},t} g_{\mathrm{PV},t}, \\
&- g_{W,t} + e_{W,t} g_{W,t} - g_{\mathrm{PV},t} + e_{\mathrm{PV},t} g_{\mathrm{PV},t} \\
&\quad \le -g_{W,t} + e_{W,t} \theta_{W,t} - g_{\mathrm{PV},t} + e_{\mathrm{PV},t} \theta_{\mathrm{PV},t} \le H_t.
\end{aligned} \tag{33}$$

Table 1: CGT operation parameters.

Unit type	g_{CPP}^{min}/MW	g_{CPP}^{max}/MW	$\Delta g_{CPP}^{\pm}$/MW	$D_{CPP,t}$/Yuan	$M_{CPP}^{on/off}$/h	Slope of segment 1/(Yuan/MW)	Slope of segment 2/(Yuan/MW)
TAURUS60	2.5	5.67	3	204.8	2	239	273.2
CENTAUR50	2	4.6	2.5	136.3	1.5	150.25	307.3
CENTAUR40	1	3.515	1.8	122.9	1	136.6	341.5

Equations (33) have obtained uncertainty constraints with the strongest robustness. If the constraint condition (16) is replaced, the most conservative system operation scheme can be obtained. However, in reality, WPP usually cannot reach the extreme condition. Therefore, wind power generation coefficient Γ_W and PV generation coefficient Γ_{PV} are introduced to describe (34), $\mathbf{\Gamma} \in [0, 1]$:

$$\begin{aligned} &-\left(g_{W,t} + e_{W,t}g_{W,t}\right) - \left(g_{PV,t} + e_{PV,t}g_{PV,t}\right) \\ &\quad \le -g_{W,t} + \Gamma_W e_{W,t}g_{W,t} - g_{PV,t} + \Gamma_{PV}e_{PV,t}g_{PV,t}, \\ &-g_{W,t} + \Gamma_W e_{W,t}g_{W,t} - g_{PV,t} + \Gamma_{PV}e_{PV,t}g_{PV,t} \\ &\quad \le -g_{W,t} + e_{W,t}\theta_{W,t} - g_{PV,t} + e_{PV,t}\theta_{PV,t} \le H_t. \end{aligned} \tag{34}$$

Combining (34) with (8), (14)–(16), and (18)–(27), a stochastic optimization model with robust adjustment coefficients is established. The proposed model could calculate the optimization scheduling scheme with different robust coefficient based on the risk attitude of policymaker.

4.3. Multiobjective Model Solving. The proposed optimization model includes two objective functions: maximizing the economic benefits and minimizing system generating fluctuation. In general, as the costs of WPP and PV generation are better, when system achieves the best economic efficiency, WPP and PV generation is relatively large, resulting in relatively large fluctuations in system output and vice versa. To achieve one optimization solution, most methods usually transfer the multiobjectives into single objective by setting different weights to every objective. So, there are two stages for solving this optimization problem.

Firstly, solve the model considering maximizing system economic benefits as the optimizing objective, and the best system economic benefits value R^{max} and system generating fluctuation at that time can be obtained.

Secondly, solve the proposed model considering minimizing system generating fluctuation as objective function, and the minimum system output N^{min} and system economic efficiency value at that time can be obtained.

Thirdly, the optimization direction of the objective function is different, so appropriate treatment is necessary in the multiobjective weighting into a single one. set α_R and α_N as weight coefficients of the maximum economic benefits and the minimum system output fluctuation. Objective functions are weighted as follows:

$$\text{obj} = \min\left\{\alpha_R \cdot \frac{R^{max} - R}{R^{max}} + \alpha_N \cdot \frac{N - N^{min}}{N^{min}}\right\}, \tag{35}$$

wherein $\alpha_R + \alpha_N = 1$. If α_N and α_R are set, optimal R and N could be achieved.

5. Simulation Analysis

In order to analyze the applicability of the proposed model in achieving the multienergy complementary system optimal operation, the study includes three parts, namely, basic data collection, optimal weights determining of the objective function, and result analysis.

5.1. Basic Data. In order to test the validity and applicability of the proposed model, a 9.6 MW wind power plant, a 6.5 MW PV unit, three CGT units, and an upper reservoir with equivalent capacity of 10 MW·h are chosen to compose a multienergy complementary system in this paper [21]. The gas turbines are, respectively, TAURUS60, CENTAUR50, and CENTAUR403 models [22]. The cost curve is divided into two segments to be linearized, and the specific parameters are shown in Table 1. The pumped storage power plant efficiency is set at 75%; the turbine and pumping regime capacities are 4 and 2 MW, respectively. The upper basin of PHSP is empty at the beginning of the day under study, and there are no constraints on the water level of the upper basin at the end of the day.

The parameters of the wind turbine are $v_{in} = 3$ m/s, $v_{rated} = 14$ m/s, and $v_{out} = 25$ m/s, and the shape parameter and scale parameter are $\varphi = 2$ and $\vartheta = 2\overline{v}/\sqrt{\pi}$ [23], respectively. The values of α and β are 0.32 and 8.14, respectively. Scenario simulation strategy proposed in [24] was further used and 50 sets of WPP and PV generation scenarios were simulated. The simulation scenarios were cut to 10 sets typical of WPP output scenarios and PV output scenarios as shown in Figure 2.

Based on the scenarios simulation results in Figure 2, select the mean output power of each scene as the WPP and PV generation input data. System load demand in a typical load day was selected according to [25], as Table 2 shows. According to [26], the load is divided into peak load (12:00–21:00) period, float load (0:00–3:00, 21:00–24:00) period, and valley load (3:00–12:00) period, and, respectively, the electricity prices are 0.77 Yuan/kW·h, 0.59 Yuan/kW·h, and 0.30 Yuan/kW·h. The grid connection prices of the CGT, WPP, and PV are 0.52 Yuan/kW·h, 0.61 Yuan/kW·h, and 1.0 Yuan/kW·h, respectively.

After inputting above basic data, the model is solved by the GAMS software using the CPLEX 11.0 linear solver from ILOG_solver [27]. The CPU time required for solving the problem of different case studies with an idea pad450

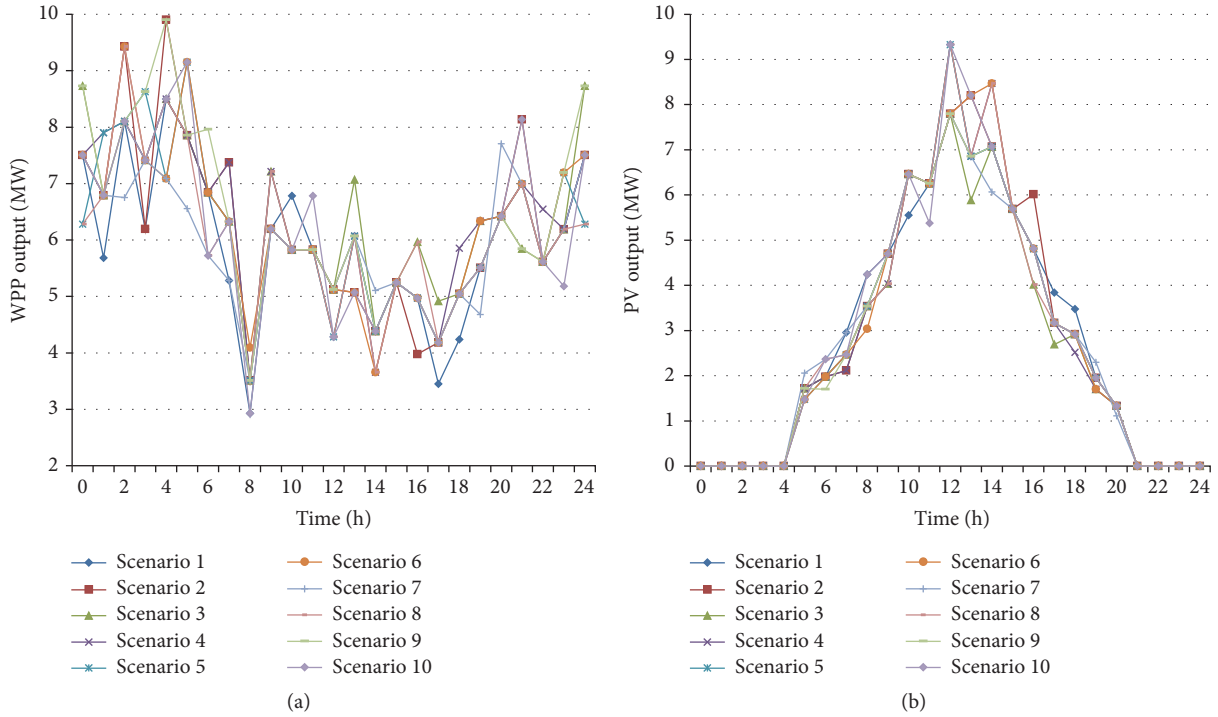

Figure 2: Scenarios simulation of WPP (a) and PV (b).

series laptop computer powered by a core T6500 processor and 4 GB of RAM under the four cases is less than 20 s. When the optimization is MILP, the GAMS software obtains a satisfactory solution quickly. Figure 3 is multiobjective joint optimization flowchart of MEHS system

5.2. Results Analysis

5.2.1. Optimal Weight Determination. The objective function weight setting will directly determine the optimal direction of system scheduling. When decision-makers pay more attention to economic benefits, α_N will be set higher with relatively higher uncertain risk of WPP and PV generation; otherwise, when decision-makers pay more attention to the uncertainty risks, α_R will be set higher with relatively lower economic benefits. To determine the optimal objective function weight, robust coefficients are set $\Gamma_W = \Gamma_{PV} = 0$ and optimization solutions of objective function R and N under different weights are estimated, as shown in Figure 4.

When $\alpha_R = 1$ and $\alpha_N = 0$, the value of MEHS system economic benefit is the optimal maximum economic benefit (R^{max}). When $\alpha_R = 0$ and $\alpha_N = 1$, the value of MEHS system WPP-PV output power fluctuating variance is the minimum fluctuating variance (N^{min}). According to Figure 4, the values of R and N both increase with the growing of α_R and rise especially quickly when α_R grows from 0.7 to 0.9, while other times both of them change little. The values of objective functions R and N keep basically equal to the optimization result of MEHS optimal economic benefit before α_R reaches 0.7 and equal to the optimization result of MEHS minimum power fluctuation optimization problem when α_R is larger than 0.9. Therefore, the comprehensive optimal results of MEHS under different α_R among 0.7~0.9 are estimated, as shown in Figure 4(b).

According to Figure 4(b), when α_R changes from 0.7 to 0.74 and 0.88 to 0.9, the values of MEHS standard deviations of economic benefit and power fluctuation increase fast; when α_R changes between 0.74 and 0.88, the standard deviations basically remained stable. That is, the results of the MEHS system will reach optimum if $\alpha_R \in [0.74, 0.88]$. Therefore, in this paper, 0.76 and 0.24 are chosen to be the optimal weights for MEHS economic objective function and the minimum objective function of power fluctuation, respectively. System decision-makers can consider their risk preference attitudes and adjust the weight coefficients α_R and α_N by choosing different α_R between 0.7 and 0.74 or between 0.88 and 0.9. Generally, decision-maker will set a smaller weighting factor α_R, while risk preference tends to set a larger α_R.

5.2.2. Validity Analysis of Robust Stochastic Optimization Theory. The WPP and PV generation uncertainties have a great impact on MEHS system operating stably. In this section, the robust stochastic optimization model for MEHS is introduced by robust stochastic optimization theory. If the prediction error $\mathbf{e} = 0.05$, separately, $\Gamma_W = \Gamma_{PV} = 0, 0.5, 0.9$, the influence of different robust coefficient settings on system scheduling results is discussed. Table 3 shows the MEHS system scheduling optimization results under different robust coefficients.

According to Table 3, after introducing robust stochastic optimization theory, with the increase of the robust coefficient, the objective function value decreases gradually. This indicates that the robust coefficient can be used to control

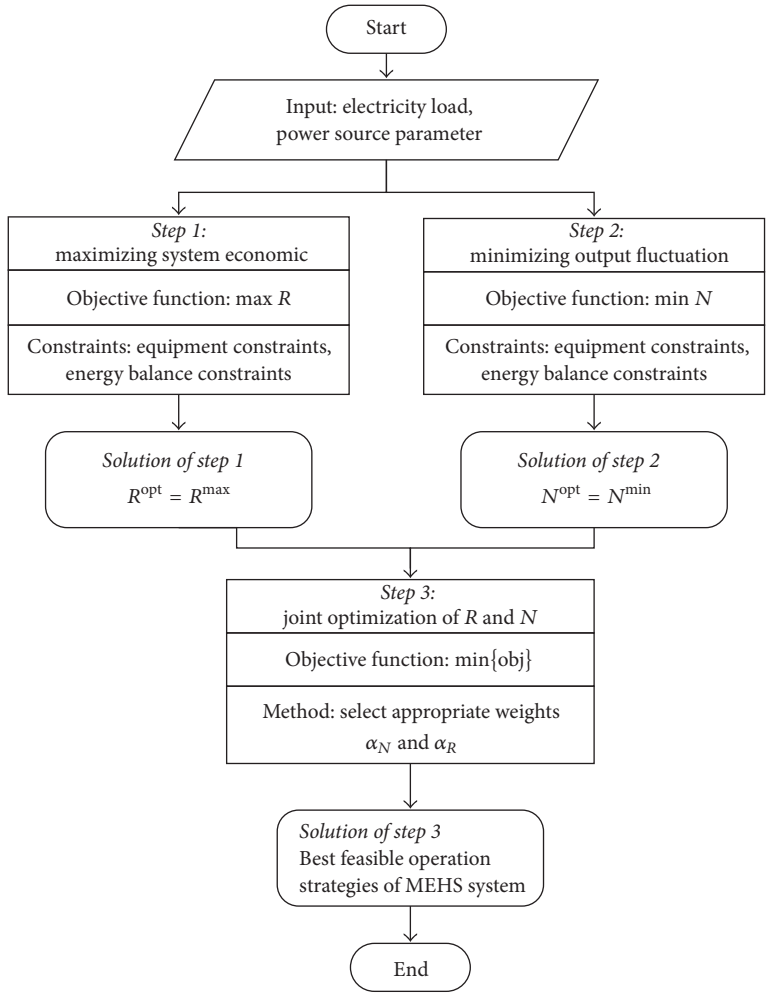

Figure 3: Multiobjective joint optimization flowchart of MEHS system.

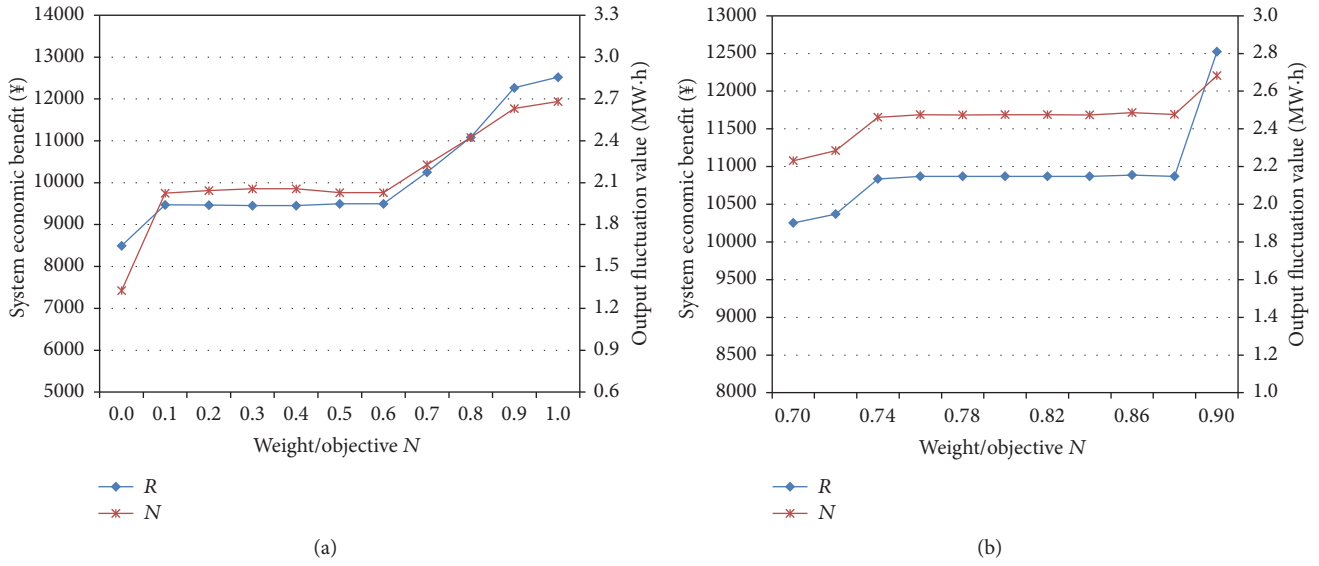

Figure 4: System economic benefits and output power fluctuation in MEHS under different (a) α_R among 0~1 and (b) α_R among 0.7~0.9.

Table 2: System load demand of WPP and PV generation output data in a typical load day (unit: MW).

Time	Load	WPP	PV
1	15.26	7.51	0
2	14.60	6.91	0
3	13.70	8.37	0
4	13.15	7.41	0
5	12.43	8.36	0
6	11.89	8.11	1.68
7	11.53	6.62	2.06
8	11.17	6.33	2.49
9	10.81	3.45	3.63
10	11.17	6.50	4.50
11	11.53	5.92	6.37
12	12.61	5.93	6.17
13	14.06	4.79	8.41
14	15.14	5.87	7.16
15	15.32	4.24	7.39
16	15.86	5.25	5.69
17	16.22	5.07	4.77
18	15.32	4.19	3.18
19	15.14	5.05	2.93
20	14.26	5.68	1.91
21	13.33	6.55	1.31
22	12.89	6.99	0
23	12.88	5.71	0
24	13.25	6.39	0

the scenery uncertainty risk by controlling the WPP and PV grid-connected electricity. Correspondingly, the MEHS economic benefit reduced gradually, but the fluctuation variance of WPP and PV output power reduced correspondingly, which indicates that system needs to bear the corresponding loss of economic benefit in avoiding risks. Conversely, if system pursues higher economic efficiency, a large scenery uncertainty risk should be taken. Compared the two scenarios, $\Gamma_W, \Gamma_{PV} = 0$ and $\Gamma_W, \Gamma_{PV} = 0.9$, the abandoned electricity of WPP and PV increased from 7.360 MW·h and 3.483 MW·h to 22.080 MW·h and 10.448 MW·h, respectively, and CGT power generation increased from 124.388 MW·h to 147.329 MW·h. This indicates system prefers to use CGT units to meet the load demand and avoid the uncertainty risk of scenery. Figure 5 shows the MEHS output power distribution under $\Gamma_W = \Gamma_{PV} = 0$.

According to Figure 5, if the uncertainty risk of WPP and PV is not considered and the weight coefficients α_N and α_R are determined, system will prefer to maximize the economic benefit. Therefore, the grid-connected generation of WPP and PV reached the maximum value, namely, 139.841 MW·h and 66.168 MW·h. The abandoned electricity of WPP and PV is 7.360 MW·h and 3.483 MW·h, respectively. Since the grid-connected generation of WPP and PV is relatively large, system will call for a larger pumped storage power station with power generation −9.706 MW·h and storage power 9.546 MW·h. At this point, system expected economic benefit

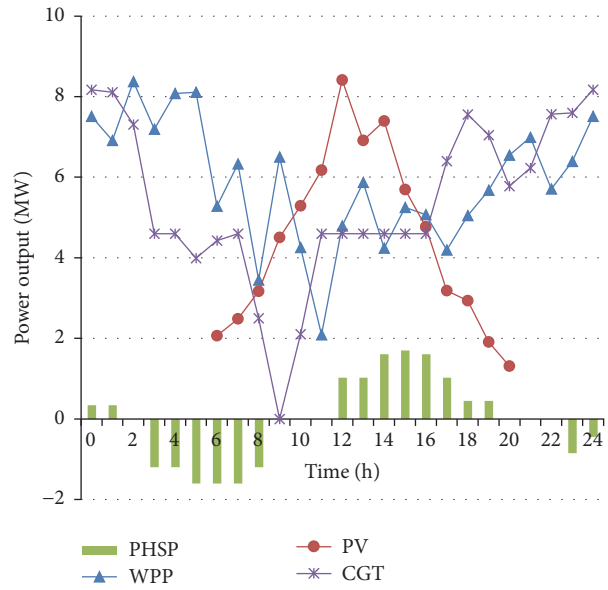

Figure 5: The MEHS output power distribution with $\Gamma_W = \Gamma_{PV} = 0$ (basic scheduling model results).

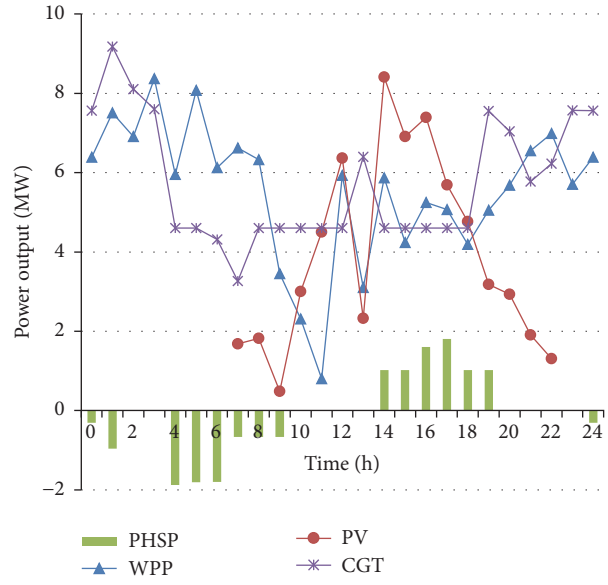

Figure 6: MEHS output power distribution with $\Gamma_W = \Gamma_{PV} = 0.5$.

reached the maximum (¥10885.20). However, system scenery output power variance reached 2.486, also the maximum, so it could not be ignored. The maximum variance means a higher system risk level. If wind speed is slow or PV intensity is not high, system will face a large power shortage risk. When system decision-makers are not willing to bear risk, WPP and PV generation will be controlled under $\Gamma_W = \Gamma_{PV} = 0.5$. Figure 6 is MEHS output power distribution with $\Gamma_W = \Gamma_{PV} = 0.5$.

Compared with Figure 5, if system decision-makers are not willing to bear operating risk, they will reduce the grid-connected generation of WPP and PV and increase

Table 3: The MEHS system scheduling optimization results with different robust coefficients.

(Γ_W, Γ_{PV})	WPP/MW·h	PV/MW·h	CGT/MW·h	PHSP/MW·h		Energy abandoned/MW·h		Objective value	
				Storage	Generation	WPP	PV	R/¥	N/MW·h
0	139.841	66.168	124.388	−9.706	9.546	7.360	3.483	10885.20	2.486
0.5	132.481	62.686	135.798	−7.726	7.487	14.720	6.965	9580.45	2.154
0.9	125.121	59.203	147.329	−5.852	5.654	22.080	10.448	8938.88	1.832

the power generation of CGT. If $\Gamma_W = \Gamma_{PV} = 0.5$, WPP, PV, and CGT generation is, respectively, 132.481 MW·h, 62.686 MW·h, and 135.798 MW·h, and abandoned WPP generation is 14.720 MW·h and 6.965 MW·h. System economic benefit reduced to ¥9580.45, the fluctuation variance of WPP output. Specifically, during the peak period, system will increase the CGT power generation. For example, at 13:00, CGT power generation increased to 6.4 MW·h; at 19:00, CGT power generation increased to 7.558 MW·h, and so on. In addition, reducing WPP and PV grid-connected generation will reduce system standby demand for pumped storage power stations. When $\Gamma_W = \Gamma_{PV} = 0.5$, the charge and discharge capacity of PHSP were −7.726 MW·h and 7.487 MW·h, respectively. This indicates that introducing robust coefficients can provide risk controlling decisions for decision-makers. If the decision-makers prefer risks, the power generation of WPP and PV will increase and CGT will reduce, and there is greater demand for PHSP reserve. On the contrary, if the decision-makers are risk-averse, the power generation of WPP and PV will reduce and CGT will increase, and the reserve demand of PHSP is relatively low.

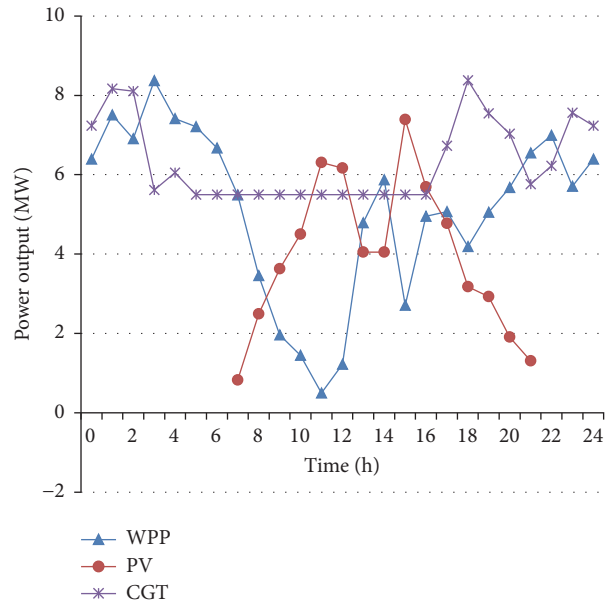

Figure 7: System scheduling operations results without PHSP.

5.2.3. Analysis on Operation Benefit of Pumped Storage Power Station. Pumped storage power stations have discharging power and pumped storage characteristics. In load valley period, pumped storage power stations can use the night low electricity price to store power and in peak period inflow water power to generate power to gain a big profit. This behavior is also conducive to smooth the load curve. In this section, the optimization effect of the pumped storage power station on MEHS system is mainly analyzed. Set $\Gamma_W = \Gamma_{PV} = 0.75$ and the prediction error coefficient is 0.9. Figures 7 and 8 show system scheduling operations results with/without PHSP are calculated respectively.

According to Figure 7, if pumped storage power stations are not considered in MEHS, the peak-shaving and reserve services of WPP and PV generation are mainly provided by CGT units. Under robust coefficients constraints, to ensure the stable system operation, WPP and PV generation reached the minimization, and the abandoned WPP and PV electricity is, respectively, 25.587 MW·h and 10.447 MW·h. Because WPP and PV generation decreased, system economic benefits dropped to ¥7793.55. The WPP and PV output fluctuating variance dropped to 1.89 MW·h at the same time, which means that though system risk level reduced, corresponding economic losses should also be borne. Furthermore, MEHS optimized operation results with PHSP were analyzed as shown in Figure 8.

According to Figure 8, if PHSP was considered in MEHS, system peak-shaving and reserve services capacity for WPP and PV power generation increased; WPP and PV power generation also increased correspondingly; abandoned WPP and PV electricity were, respectively, 1 × 7.664 MW·h and 8.358 MW·h. With the increasing of wind and photovoltaic power generation, MEHS economic benefits increased to ¥7954.29 and the WPP and PV output power fluctuating variance also increased to 1.84 MW·h. The results indicate that PHSP can improve MEHS to absorb WPP and PV generation, reduce abandoned WPP and PV electricity, and enhance MEHS economic efficiency. At the same time, the pumped storage power station can match the WPP and PV output power considering the peak-valley condition of load curve, which can reduce the output fluctuation and reduce the MEHS operation risks. Table 4 shows the MEHS system scheduling operations results with/without PHSP.

According to Table 4, PHSP can optimize the operation strategy considering the peak-valley distribution and the actual power generation capacity of WPP and PV. After considering PHSP, the peak load decreased to 14.18 MW, the valley increased to 11.05 MW, and peak to valley ratio reduced to 1.50, meaning system economic efficiency and risk level are better than before. This indicates that PHSP can smooth the electricity load curve and reduce the peak-valley ratio. This process can also increase WPP and PV grid-connected power and reduce the amount of abandoned wind and photovoltaic power. The MEHS system economic benefits can be improved and the MEHS system operation

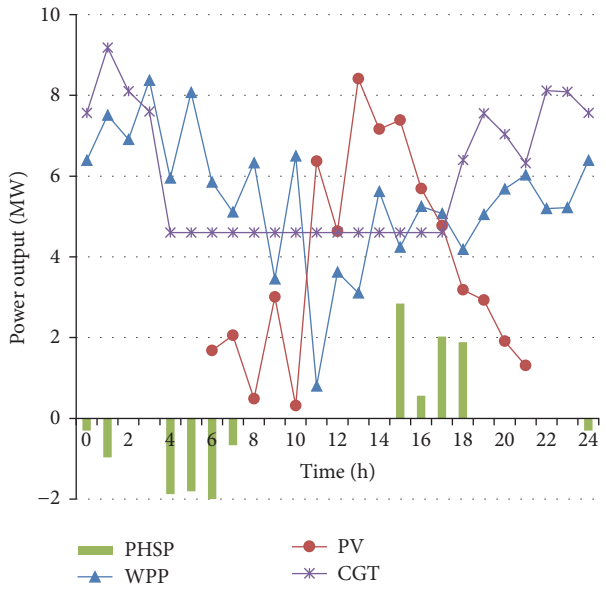

Figure 8: System optimized operation results with PHSP.

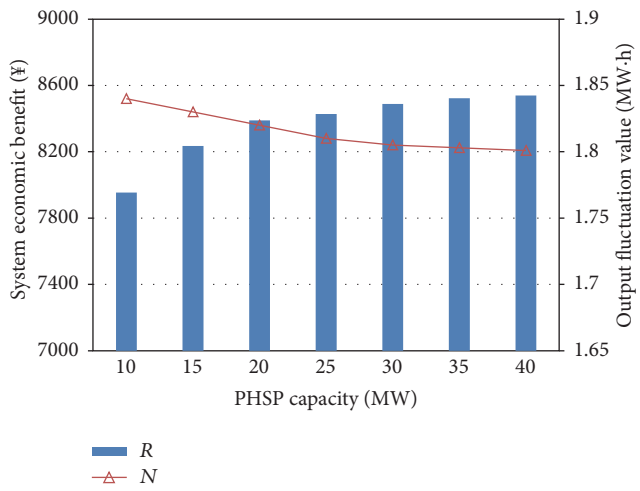

Figure 9: MEHS system scheduling optimization results with different PHSP capacities.

risk level can be reduced though the process. Furthermore, the MEHS system scheduling optimization results under different PHSP capacities were quantitatively analyzed, and the MEHS economic benefits and risk level under different PHSP capacities were discussed as shown in Figure 9.

According to Figure 9, with the increasing of PHPS grid-connected capacity, MEHS system economic benefits increased correspondingly; the WPP and WPP and PV output fluctuation variance in MEHS reduced gradually, which means that PHSP can provide peak-shaving and reserve service for MEHS system. This process can also promote the WPP and PV grid-connected power and improve the MEHS economic efficiency and reduce the operational risk level. When the PHSP capacity is 40 MW, the MEHS economic benefit reached ¥8738.88 and the fluctuation variance of WPP and PV output power fluctuation dropped to 1.78 MW·h. Compared with PHSP capacity of 10 MW, the economic benefit of MEHS increased by 7.34% and the risk level reduced by 2.16%. However, when the PHSP capacity reaches 25 MW (WPP and PV installed capacity and PHPS capacity ratio is about 1 : 1.3), the economic efficiency and risk level of MEHS reached the inflection point. When the proportion exceeds 1 : 1.3, the increase of PHSP capacity has a relatively weak optimizing impact on MEHS, indicating PHSP peak-shaving and reserve capacity is sufficient and the WPP and PV generation has basically reached the upper limit. Overall, PHSP can improve the economic efficiency and reduce the risk level of MEHS system, but it is necessary to set reasonable PHSP capacities for specific WPP and PV installed capacity.

5.3. Sensitivity Analysis. In this paper, based on WPP and PV predicted generation power, the robust coefficients are introduced to characterize the WPP and PV generation uncertainties. The rationality of robust coefficients and prediction error coefficients setting is significant in determining optimal scheduling scheme. In this section, the results of system optimization and CGT units output under different robust coefficients and prediction errors are discussed, respectively. Figure 10 shows the MEHS operating economic benefit (a) and risk level (b) under different robust coefficients and prediction errors.

According to Figure 10, with the increase of the robust coefficients and the prediction error coefficients, the MEHS system economic efficiency and the risk level decreased, which indicates that system decision-makers will reduce WPP and PV grid-connected generation to reduce the uncertainty risk. The corresponding extra benefits of WPP and PV would be lost, but the MEHS overall risk level reduced. When robust coefficient is less than or equal to 0.5, the increase of the robust coefficient had a great impact on the optimizing target. On the contrary, when the robust coefficient is bigger than 0.5, the impact is small. Similarly, when the prediction error is less than or equal to 0.5, the increase of the error coefficient had a great influence on the objective function. When the error coefficient is bigger than 0.5, the influence is small. This indicates that when the robust coefficient and the prediction error coefficient are higher than 0.5, system scheduling scheme is close to the most conservative operation scheme. In order to meet system load balance, necessary wind and photovoltaic power generation need to be absorbed. Higher economic benefits could be obtained by loosening robust coefficient or increasing the power prediction accuracy. Figure 11 shows CGT units generation under different robust coefficients and the prediction errors.

According to Figure 11, with the increase of the robust coefficient and the predicting error coefficient, MEHS use CGT to generate more electricity so as to reduce WPP and PV generation and system operation risk. Specifically, with the predicting error coefficient increasing, the CGT units output shows a three-segment distribution. When the predicting error coefficient is between 0.3 and 0.7, system quickly calls the CGT to generate power, which means larger error caused system calling CGT units with faster startup-shutdown speed to meet load demand. When the coefficient is less than 0.3, system could call PHSP to meet the uncertain demand of

Table 4: MEHS scheduling operations results with/without PHSP.

	WPP/MW·h	PV/MW·h	CGT/MW·h	PHSP/MW·h		Load curve			Objective function	
				Power storage	Power generation	Peak load/MW	Valley load/MW	Peak-valley ratio	R/¥	N/MW·h
Without PHSP	135.01	108.21	59.20	0	0	16.22	10.81	1.50	7793	1.89
With PHSP	132.81	123.15	61.29	−7.93	7.32	14.18	11.05	1.28	7954	1.84

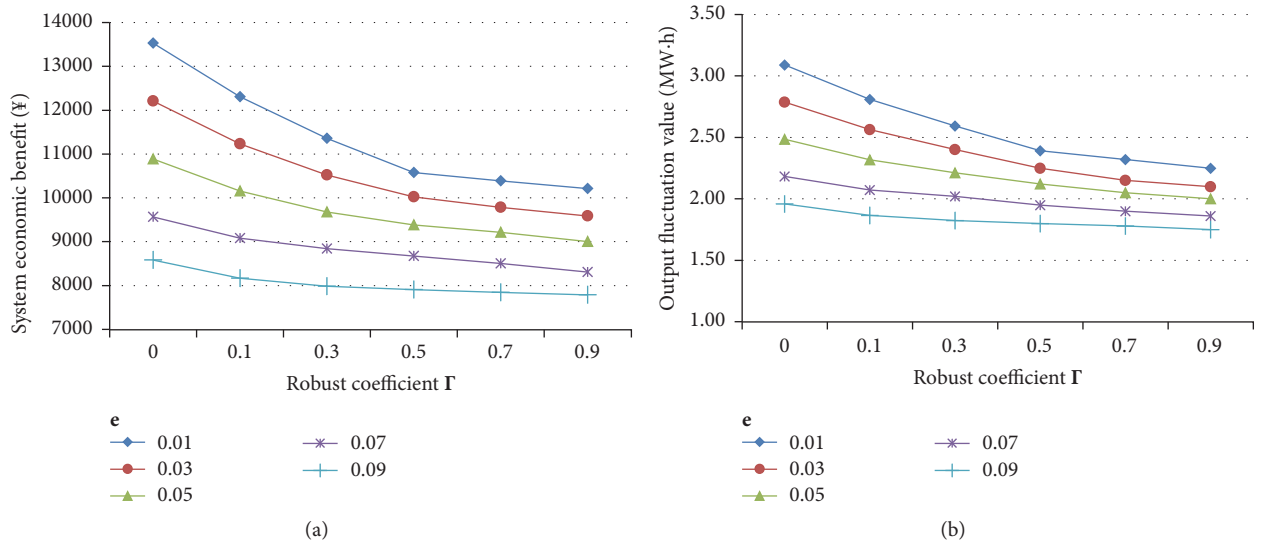

Figure 10: MEHS operating economic benefits (a) and risk levels (b) under different robust coefficients and prediction errors.

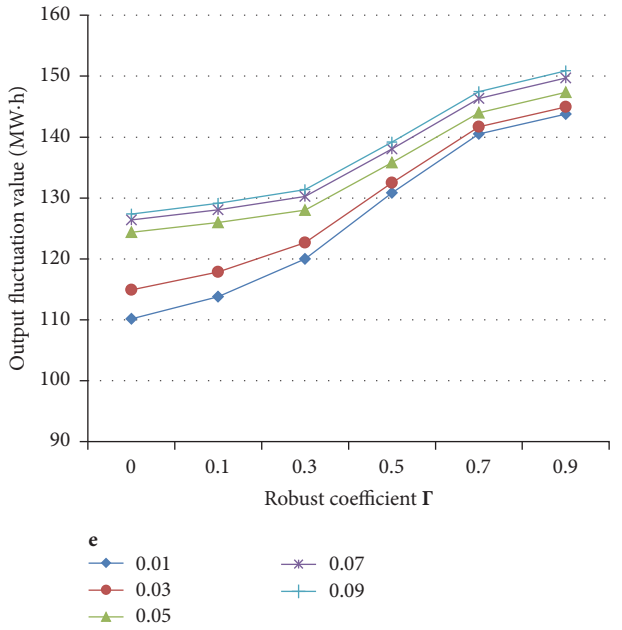

Figure 11: CGT with different robust coefficients and the prediction errors.

WPP and PV. Therefore, the CGT call frequency is relatively slow. When the coefficient is higher than 0.7, due to system having made full use of CGT generating power, the remaining predicting error power cannot be satisfied by CGT. MEHS needs other power suppliers to meet system load demand. Similarly, when the robust coefficient is less than or equal to 0.5, the increase of robust coefficient has a great effect on the optimizing target. On the contrary, when robust coefficient is higher than 0.5, the effect is little. This indicates that the robust coefficient provides risk controlling methods for decision-makers. In order to pursue higher economic efficiency and economic risk level, decision-makers should improve the power forecasting accuracy. Reasonable robust coefficients should be set with their risk-bearing capacity to win extra economic benefits.

6. Conclusions

In this paper, WPP, PV PHSP, and CGT units are integrated as MEHS system. The robust stochastic optimization theory is introduced to describe the uncertainties of WPP and PV generation. A multiobjective scheduling optimization mode for MEHS considering uncertainty is put forward. Firstly, in order to characterize the uncertainties of WPP and PV generation, an uncertainty description method based on the power prediction results is established. Secondly, robust coefficients are introduced to transform the constraints with uncertain variables. The stochastic constraint conditions are obtained, and freely adjustable risk controlling methods are provided for decision-makers. Finally, the validity and validity of the

proposed model are proved by examples analysis. The results show the following:

(1) Integrating WPP, PV, PHSP, and CGT into MEHS system can make full use of different energy generation characteristics and realize the multienergy complementary features. PHSP will generate power in peak load periods and pumped storage in valley periods. When PHSP is insufficient to meet peak-shaving and reserve demand, CGT units will be called to meet system supply-demand balance constraints. In general, multienergy complementary system can make system operation stable and increase economic efficiency and lower risk levels.

(2) Robust stochastic optimization theory can effectively overcome the uncertainty of WPP and PV. Risk controlling methods can be provided for decision-makers with different risk preferences. When decision-makers prefer to take a risk, robust coefficient is relatively low. More WPP and PV generation are absorbed, and more economic benefits are gained. On the contrary, higher robust coefficient will lower WPP and PV generation, and CGT units are called to meet load demand to reduce system risk level.

(3) PHSP can optimize the status of pumped storage power considering the load supply-demand situation and the actual available output of WPP and PV. PHSP realizes the peak-shaving and valley filling of load curve and provides more space for WPP and PV and enhances the economic benefits. At the same time, PHSP converts working condition rapidly to overcome the uncertainty of WPP and PV generation which can reduce generation output fluctuation and minimize system operation risk.

(4) In this paper, clean energy generating units, conventional energy generation units, and pumped storage units in generation side are mainly considered in constructing multiobjective complementary system. In the future, with the continuous maturity and upgrading of intelligent communication and information technology, demand response in the user side will be considered to achieve the optimization effect in both generation side and the user side and improve the operating efficiency of MEHS system.

Conflicts of Interest

The authors declare that there are no conflicts of interest regarding the publication of this paper.

Acknowledgments

This paper is supported by the National Science Foundation of China (Grant no. 71271081).

References

[1] L. Ju, Z. Tan, H. Li, Q. Tan, X. Yu, and X. Song, "Multi-objective operation optimization and evaluation model for CCHP and renewable energy based hybrid energy system driven by distributed energy resources in China," *Energy*, vol. 111, pp. 322–340, 2016.

[2] F. Klumpp, "Comparison of pumped hydro, hydrogen storage and compressed air energy storage for integrating high shares of renewable energies—potential, cost-comparison and ranking," *Journal of Energy Storage*, vol. 8, pp. 119–128, 2016.

[3] K. Kusakana, "Optimal scheduling for distributed hybrid system with pumped hydro storage," *Energy Conversion and Management*, vol. 111, no. 1, pp. 253–260, 2016.

[4] K. Geetha, V. D. Sharmila, and K. Keerthivasan, "Design of economic dispatch model for gencos with thermal and wind powered generators," *International Journal of Electrical Power and Energy Systems*, vol. 68, no. 7, pp. 222–232, 2015.

[5] C. H. Peng, H. J. Sun, J. F. Guo, and G. Liu, "Dynamic economic dispatch for wind-thermal power system using a novel bi-population chaotic differential evolution algorithm," *International Journal of Electrical Power and Energy Systems*, vol. 42, no. 1, pp. 119–126, 2012.

[6] R. Dufo-López, J. L. Bernal-Agustín, J. M. Yusta-Loyo et al., "Multi-objective optimization minimizing cost and life cycle emissions of stand-alone PV-wind-diesel systems with batteries storage," *Applied Energy*, vol. 88, no. 11, pp. 4033–4041, 2011.

[7] M. J. Ghadi, A. I. Karin, A. Baghramian et al., "Optimal power scheduling of thermal units considering emission constraint for GENCOs' profit maximization," *International Journal of Electrical Power and Energy Systems*, vol. 82, pp. 124–135, 2016.

[8] S. V. Papaefthymiou, E. G. Karamanou, S. A. Papathanassiou, and M. P. Papadopoulos, "A wind-hydro-pumped storage station leading to high RES penetration in the autonomous island system of Ikaria," *IEEE Transactions on Sustainable Energy*, vol. 1, no. 3, pp. 163–172, 2010.

[9] M. Parastegari, R.-A. Hooshmand, A. Khodabakhshian, and Z. Forghani, "Joint operation of wind farms and pump-storage units in the electricity markets: modeling, simulation and evaluation," *Simulation Modelling Practice and Theory*, vol. 37, pp. 56–69, 2013.

[10] Y. Gebretsadik, C. Fant, K. Strzepek, and C. Arndt, "Optimized reservoir operation model of regional wind and hydro power integration case study: zambezi basin and South Africa," *Applied Energy*, vol. 161, pp. 574–582, 2016.

[11] R. Karki, P. Hu, and R. Billinton, "Reliability evaluation considering wind and hydro power coordination," *IEEE Transactions on Power Systems*, vol. 25, no. 2, pp. 685–693, 2010.

[12] T. K. A. Brekken, A. Yokochi, A. von Jouanne, Z. Z. Yen, H. M. Hapke, and D. A. Halamay, "Optimal energy storage sizing and control for wind power applications," *IEEE Transactions on Sustainable Energy*, vol. 2, no. 1, pp. 69–77, 2011.

[13] Á. J. Duque, E. D. Castronuovo, I. Sánchez, and J. Usaola, "Optimal operation of a pumped-storage hydro plant that compensates the imbalances of a wind power producer," *Electric Power Systems Research*, vol. 81, no. 9, pp. 1767–1777, 2011.

[14] T. Ma, H. Yang, L. Lu, and J. Peng, "Pumped storage-based standalone photovoltaic power generation system: Modeling and techno-economic optimization," *Applied Energy*, vol. 137, no. 1, pp. 649–659, 2015.

[15] F. Petrakopoulou, A. Robinson, and M. Loizidou, "Simulation and analysis of a stand-alone solar-wind and pumped-storage hydropower plant," *Energy*, vol. 96, no. 1, pp. 676–683, 2016.

[16] M. Z. Oskouei and A. Sadeghi Yazdankhah, "Scenario-based stochastic optimal operation of wind, photovoltaic, pump-storage hybrid system in frequency-based pricing," *Energy Conversion and Management*, vol. 105, no. 15, pp. 1105–1114, 2015.

[17] S. Chakraborty and T. Okabe, "Robust energy storage scheduling for imbalance reduction of strategically formed energy balancing groups," *Energy*, vol. 114, pp. 405–417, 2016.

[18] A. M. Foley, P. G. Leahy, K. Li, E. J. McKeogh, and A. P. Morrison, "A long-term analysis of pumped hydro storage to firm wind power," *Applied Energy*, vol. 137, pp. 638–648, 2015.

[19] H. Y. Jiang, *Mahmoud Comparative Study of Numerical Methods and Swarm Intelligence Algorithms on Optimizing Low Wind Speed Distribution Models*, Lanzhou University, Lanzhou, China, 2015.

[20] M. Yu, Y. Yu, and R. Tang, "Angular distribution of annual collectible radiation on solar cells of CPC based photovoltaic systems," *Solar Energy*, vol. 135, no. 10, pp. 827–839, 2016.

[21] E. Barbour, I. A. G. Wilson, J. Radcliffe, Y. Ding, and Y. Li, "A review of pumped hydro energy storage development in significant international electricity markets," *Renewable and Sustainable Energy Reviews*, vol. 61, no. 8, pp. 421–432, 2016.

[22] S. Yu, Z. H. Wei, and G. Q. Sun, "A bidding model for a virtual power plant considering uncertainties," *Automation of Electric Power System*, vol. 38, no. 22, pp. 44–49, 2014.

[23] L. Ju, Z. Tan, J. Yuan, Q. Tan, H. Li, and F. Dong, "A bi-level stochastic scheduling optimization model for a virtual power plant connected to a wind-photovoltaic-energy storage system considering the uncertainty and demand response," *Applied Energy*, vol. 171, pp. 184–199, 2016.

[24] N. Amjady, J. Aghaei, and H. A. Shayanfar, "Stochastic multi-objective market clearing of joint energy and reserves auctions ensuring power system security," *IEEE Transactions on Power Systems*, vol. 24, no. 4, pp. 1841–1854, 2009.

[25] Y. Zou and L. Yang, "Synergetic dispatch models of a wind/PV/hydro virtual power plant based on representative scenario set," *Power System Technology*, vol. 39, no. 7, pp. 1855–1859, 2015.

[26] Z. F. Tan, L. W. Ju, H. H. Li et al., "A two-stage scheduling optimization model and solution algorithm for wind power and energy storage system considering uncertainty and demand response," *International Journal of Electrical Power & Energy Systems*, pp. 1057–1069, 2014.

[27] Z. Tan, L. Ju, B. Reed et al., "The optimization model for multi-type customers assisting wind power consumptive considering uncertainty and demand response based on robust stochastic theory," *Energy Conversion and Management*, vol. 105, pp. 1070–1081, 2015.